

GPF-NET: GATED PROGRESSIVE FUSION LEARNING FOR POLYP RE-IDENTIFICATION

Suncheng Xiang^{1#}, Xiaoyang Wang^{2#}, Junjie Jiang³, Hejia Wang¹, Dahong Qian¹

¹Shanghai Jiao Tong University, ²Peking University, ³Shanghai Fifth People's Hospital

ABSTRACT

Colonoscopic Polyp Re-Identification aims to match the same polyp from a large gallery with images from different views taken using different cameras, which plays an important role in the prevention and treatment of colorectal cancer in computer-aided diagnosis. However, the coarse resolution of high-level features of a specific polyp often leads to inferior results for small objects where detailed information is important. To address this challenge, we propose a novel architecture, named Gated Progressive Fusion network, to selectively fuse features from multiple levels using gates in a fully connected way for polyp ReID. On the basis of it, a gated progressive fusion strategy is introduced to achieve layer-wise refinement of semantic information through multi-level feature interactions. Experiments on standard benchmarks show the benefits of the multimodal setting over state-of-the-art unimodal ReID models, especially when combined with the specialized multimodal fusion strategy. The code is publicly available at <https://github.com/JeremyXSC/GPF-Net>.

Index Terms— Colonoscopic polyp re-Identification, modal representation, gated progressive fusion

1. INTRODUCTION

Colonoscopic polyp re-identification (Polyp ReID) aims to match a specific polyp in a large gallery with different cameras and locations, which has been studied intensively due to its practical importance in the prevention and treatment of colorectal cancer in the computer-aided diagnosis. With the development of deep convolution neural networks and the availability of video re-identification dataset, video retrieval methods have achieved remarkable performance in a supervised manner [1], where a model is trained and tested on different splits of the same dataset. However, in practice, manually labeling a large diversity of pairwise polyp area data is time-consuming and labor-intensive when directly deploying polyp ReID system to new hospital scenarios [2, 3]. Nevertheless, when compared with the conventional ReID, polyp ReID is confronted with more challenges in some aspects: **1) from the model perspective:** traditional object

[#] indicates contributed equally. This work was partially supported by the National Natural Science Foundation of China under Grant No.62301315.

ReID methods learn the unimodal representation by greedily “pre-training” several layers of features on the basis of visual samples, while ignore to explore complementary information from different modalities, and **2) from the data perspective**, polyp ReID will encounter many challenges such as variation in terms of backgrounds, viewpoint, and illumination, *etc.*, which poses great challenges to the clinical deployment of deep model in real-world scenarios.

Our key innovation lies in the Gated Progressive Fusion Network (GPF-Net), which combines a gated attention mechanism inspired by Gated Multimodal Units with a progressive fusion strategy. Unlike traditional single-stage fusion, which iteratively refines multimodal representations through four stacked gated fusion layers. On the contrary, our approach addresses the limitations of prior methods by capturing both low-level discriminative patterns and high-level semantic correlations across modalities. Extensive experiments on polypus dataset demonstrate that GPF-Net achieves state-of-the-art performance, outperforming existing methods by significant margins in mAP and Rank-1 accuracy. Our work not only advances the field of polyp ReID but also provides insights into effective multimodal fusion strategies for medical image retrieval tasks.

In summary, the main contributions of this paper can be summarized as follows: 1) We construct a multimodal feature fusion framework named GPF-Net majoring in multi-scale feature extraction for polyp ReID. 2) A dynamic gating progressive fusion mechanism is introduced to achieve layer-wise refinement of semantic information through multi-level feature interactions, which can adaptively adjust modality weights based on visual content, then enhancing feature discriminability. 3) Experiments demonstrate that the proposed method significantly outperforms existing approaches across multiple metrics, while maintaining competitive computational complexity than current polyp ReID methods.

2. METHODOLOGY

2.1. Preliminary

We begin with a formal description of the colonoscopic polyp re-identification (Polyp ReID) problem. Assuming that we are given a source domain \mathcal{D} , which contains its own image-label pairs $\mathcal{D} = \{(x_i, y_i)\}_{i=1}^N$ of colonoscopic videos, where

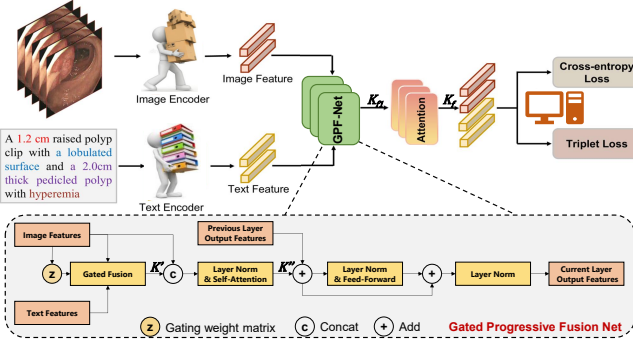


Fig. 1. The overall architecture of our proposed GPF-Net method, which consists of gated progressive fusion net and self-attention layers.

N is the number of images in the source domain \mathcal{D} . Each sample $\mathbf{x}_i \in \mathcal{X}$ is associated with an identity label $y_i \in \mathcal{Y} = \{1, 2, \dots, M\}$, where M is the number of identities in the source domain \mathcal{D} . The goal of this work is to leverage labeled source training polyp samples to learn the discriminative embeddings of the target testing set on polyp ReID task.

2.2. Our Proposed GPF-Net Framework

The overall architecture of our model is illustrated in Figure 1, which primarily consists of: (1) a visual-textual feature extraction module, and (2) a two-stage feature fusion module. Specially, the model in this study employs a pre-trained ResNet-50 as the image feature extraction network. Specifically, given a polyp image with dimensions $224 \times 224 \times 3$, after normalization, the image feature extraction network encodes the input into a 1×2048 -dimensional feature vector. This vector is then dimensionally reduced to obtain a 512 -dimensional image feature $I \in \mathbb{R}^{d_v}$. For text feature extraction, the study utilizes a pre-trained ALBERT model [4] as the text feature extraction network. Given a colonoscopy report description containing n tokens, ALBERT encodes it into an $n \times 768$ -dimensional text feature $T \in \mathbb{R}^{d_t}$.

To effectively integrate visual and textual features, we propose a Gated Progressive Fusion Network combined with a dual-stage fusion strategy based on a Transformer encoder. Specially, the image feature I and the text feature T are concatenated, and positional encoding is applied to this concatenated result to obtain the preliminary fused feature $[I, T] \in \mathbb{R}^{2d}$. Subsequently, the extracted feature $[I, T]$ is fed into a 4-layer gated progressive fusion network. Through the Gating Progressive Fusion mechanism, the contribution weights of visual and textual features are dynamically adjusted. Additionally, the progressive fusion approach avoids a single-step direct fusion of the two modalities, ultimately generating the intermediate feature K_{f1} through multiple rounds of interactive fusion between the two modalities.

Finally, the fused feature K_f output by Transformer is employed to compute the model loss for optimizing the model θ . Regarding the design of the specific loss function, this work considers that many previous studies [5] have demonstrated the importance of employing multiple loss functions for training robust and generalizable ReID models. Therefore, during training, we adopt identity loss and triplet loss as the optimization objectives of our model. Specifically, the triplet loss function aims to reduce the feature distance between similar polyp images while increasing the feature distance between dissimilar ones. Meanwhile, the identity loss function enhances the model's ability to recognize and classify polyp categories.

2.3. Dynamic Gating Progressive Fusion Mechanism

On the basis of GPF-Net, we also introduce the gating progressive fusion mechanism to achieve layer-wise refinement of semantic information through multi-level feature interactions. First, the image features I , obtained through the visual feature extraction network ResNet-50 [6], are passed through a fully connected layer to produce an intermediate vector $W_z \cdot I$, where W_z is a learnable matrix. Subsequently, this intermediate vector $W_z \cdot I$ is processed through a Sigmoid activation function, thereby generating the gating weight matrix z , shown in Eq. 1. Finally, the generated gating weight matrix z is utilized to adjust the proportions of the image and text modalities in the fused features, as following:

$$z \leftarrow \text{Sigmoid}(W_z \cdot I) \quad (1)$$

$$K' \leftarrow z * T + (1 - z) * I \quad (2)$$

$$K'' = \text{LayerNorm}([I, K']) \quad (3)$$

where K' represents the features after gated weighted fusion. Furthermore, in contrast to traditional gated fusion methods that directly adopt the weighted vector as the fused feature, we leverage the characteristics of the Multi-Head Attention layer to map the fused features into a higher-dimensional feature space, which enables the thorough mining and extraction of deep semantic information from the fused vectors, resulting in the final fused feature K'' , as shown in Eq. 3. To strike a balance between fully extracting features for accurate polyp ReID and reducing model parameters and computational load to maintain model lightness, we also employ an 8-head self-attention mechanism in the 4-layer gated progressive fusion network, while utilizing a 4-head self-attention mechanism in the final 4-layer Transformer encoder.

3. EXPERIMENTS

3.1. Datasets and Evaluation Metric

We conduct experiments on several large-scale public datasets, which include Colo-Pair [2], Market-1501 [7], DukeMTMC-reID [8] and CUHK03 dataset [9]. We follow the standard

evaluation protocol [7] used in the ReID task and adopt mean Average Precision (mAP) and Cumulative Matching Characteristics (CMC) at Rank-1, Rank-5, and Rank-10 for performance evaluation on downstream ReID task.

3.2. Implementation details

Following the training procedure in [3], we adopt the common methods such as random flipping and random cropping for data augmentation and employ the Adam optimizer with a weight decay co-efficient of 1×10^{-5} and 1×10^{-7} for parameter optimization. Besides, we adopt the ID loss and triplet loss functions to train the model for 180 iterations, and the cosine distance is also adopted to calculate the similarity of polyp features in the dataset for the task of polyp ReID. In addition, the batch size M_{batch} for training is set to 64. All the experiments are performed on the PyTorch framework with one Nvidia GeForce RTX 4090 GPU on a server equipped with an AMD EPYC 7713 64-Core Processor.

3.3. Comparison with State-of-the-Arts

Colonoscopic Polyp Re-Identification. In this section, we compare our proposed method with the state-of-the-art algorithms, including: (1) transformer based (soft attention) models ViT [10], Colo-SCRL [2] and VT-ReID [3]; (2) knowledge distillation-based methods, such as CgS^c, FgAttS_A^f and FgBinS_B^f [11]; (3) feature level based methods, such as ViSiL [12], CoCLR [13], TCA [14], CVRL [15]. According to the results in Table 1, we can easily observe that our method shows the clear performance superiority over other state-of-the-arts with significant Rank-1 and mAP advantages. For instance, when compared to the knowledge distillation-based network FgAttS_A^f [11], our model improves Rank-1 accuracy by **+70.5%** (80.2 vs. 9.7). Besides, GPF-Net also surpasses recent transformer based (soft attention) models ViT [10], Colo-SCRL [2] and VT-ReID [3]. Specially, our method outperforms the second best model DMCL [16] by **+22.5%** (68.9 vs. 46.4) and **+25.9%** (80.2 vs. 54.3) in terms of mAP and Rank-1 accuracy, respectively. The superiority of our proposed method can be largely contributed to the visual-text representation extracted by our GPF-Net during multiple collaborative training, as well as the dynamic multimodal feature fusion strategy, which is beneficial to learn a more robust and discriminative model in polyp ReID tasks.

Person Re-Identification. To further prove the effectiveness of our method on other related object ReID tasks, we also compare our GPF-Net with existing methods in Table 2. we can easily observe that our method can achieve the state-of-the-art performance on Market-1501, DukeMTMC-reID and CUHK03 datasets with considerable advantages respectively. For example, our GPF-Net method can achieve a mAP/Rank-1 performance of 93.1% and 98.1% respectively on Market-1501 dataset, leading **+1.8%** improvement of Rank-1 accu-

Table 1. Performance comparison with state-of-the-art methods on Colo-Pair dataset. **Bold** indicates the best and underline the second best.

Method	Venue	Video Retrieval ↑			
		mAP	Rank-1	Rank-5	Rank-10
ViSiL [12]	ICCV 19	24.9	14.5	30.6	51.6
CoCLR [13]	NIPS 20	16.3	6.5	22.6	33.9
TCA [14]	WCAV 21	27.8	16.1	35.5	53.2
ViT [10]	CVPR 21	20.4	9.7	30.6	43.5
CVRL [15]	CVPR 21	23.6	11.3	32.3	53.2
CgS ^c [11]	IJCV 22	21.4	8.1	35.5	45.2
FgAttS _A ^f [11]	IJCV 22	23.6	9.7	40.3	50.0
FgBinS _B ^f [11]	IJCV 22	21.2	9.7	32.3	48.4
Colo-SCRL [2]	ICME 23	31.5	22.6	41.9	58.1
VT-ReID [3]	ICASSP 24	37.9	23.4	44.5	60.1
DMCL [16]	arXiv 24	46.4	54.3	57.9	60.4
GPF-Net	Ours	68.9	80.2	89.6	91.6

Table 2. Performance comparison with other methods on Person ReID datasets. **Bold** indicates the best and underline the second best.

Method	Market-1501		DukeMTMC-reID		CUHK03	
	mAP	Rank-1	mAP	Rank-1	mAP	Rank-1
PCB [17]	81.6	93.8	69.2	83.3	57.5	63.7
MHN [18]	85.0	95.1	77.2	77.3	76.5	71.7
ISP [19]	88.6	95.3	80.0	89.6	71.4	75.2
CBDB [20]	85.0	94.4	74.3	87.7	72.8	75.4
C2F [21]	87.7	94.8	74.9	87.4	84.1	81.3
NFormer [22]	91.1	94.7	<u>83.5</u>	89.4	74.7	77.3
MGN [23]	86.9	95.7	78.4	88.7	66.0	66.8
SCSN [24]	88.3	92.4	79.0	91.0	81.0	84.7
VT-ReID [3]	88.1	93.8	79.2	<u>92.6</u>	85.3	88.3
DMCL [16]	92.1	<u>96.3</u>	87.6	<u>93.5</u>	86.5	<u>89.7</u>
GPF-Net	93.1	98.1	74.4	74.1	88.2	98.9

racy when compared to the second best method DMCL [16]. In addition, our GPF-Net method can also obtain the improvement of **+9.2%** in terms of Rank-1 accuracy on CUHK03 dataset when compared to the DMCL [16]. Unfortunately, we also observe the inferiority of GPF-Net on DukeMTMC-reID, we suspect that this is due to the imbalanced distribution in the Duke dataset which causes the model to overfit the features of high-frequency samples while overlooking the uniqueness of low-frequency ones, thereby compromising the fairness and comprehensiveness of feature extraction.

3.4. Ablation Studies

Effectiveness of Multimodal Feature Fusion GPF-Net Framework: Firstly, from the quantitative aspect, we evaluate the effectiveness of multimodal feature fusion GPF-Net framework. As illustrated in Table 3, when adopting our gated progressive fusion framework, results show that mAP accuracy improves significantly from 27.94% to 68.86% on

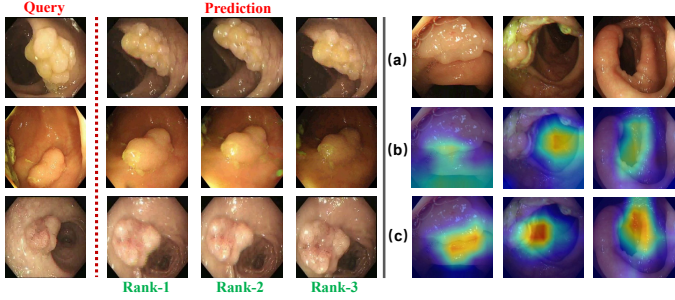


Fig. 2. Visualization of ranking results (left) and attention maps(right): (a) Original images; (b) CNN-based training method without text information; (c) Our gated progressive fusion strategy.

Colo-Pair dataset with visual-text induction. Additionally, similar improvements can also be easily observed in terms of Rank-1, Rank-5 evaluation metrics, leading to +60.64% and +50.49% respectively. These results prove that gated progressive fusion paradigm has a direct impact on downstream polyp ReID task.

Secondly, from the qualitative aspect, we also give some qualitative results of our proposed gated progressive fusion framework on multimodal polyp scenarios. For example, Fig. 2 provides some ranking results and attention visualization of GPF-Net. To be more specific, we can obviously observe that our model attends to relevant image regions or discriminative parts for making polyp predictions, indicating that GPF-Net can greatly help the model learn more global context information and meaningful visual features with better multimodal understanding, which provides the possibility to discover deeper layer of neural network and more representative features from images automatically.

Effectiveness of Dynamic Gating Progressive Fusion Mechanism:

In this section, we proceed to evaluate the effectiveness of dynamic multimodal training strategy by testing whether text modality or image modality matters. According to Table 3, our dynamic multimodal training strategy GPF-Net with text representation (GPF-Net w/ text) can lead to a significant improvement in Rank-1 of +1.1% on Colo-Pair dataset when compared with baseline setting. Furthermore, when adopting image representation, our method (GPF-Net w/ image) can obtain a remarkable performance of 59.91% in terms of mAP accuracy, leadig a significant improvement of **+30.37%** when compared to GPF-Net w/ text. In particular, we find that the missing low-level features can be fused into each feature level in the pyramid, which indicates that our module can well handle small and thin polyps in complex medical scenarios. To sum up, the effectiveness of the dynamic multimodal training strategy can be largely attributed to that it enhances the discrimination capability of collaborative networks during multimodal representation learning,

Table 3. Ablation study of different pre-training settings from Colo-Pair dataset. Note that the pre-trained model is then fine-tuned on dataset for downstream polyp ReID task.

Pre-training	Text data	Image data	Colo-Pair \uparrow		
			mAP	Rank-1	Rank-5
Baseline	\times	\times	27.94	19.53	39.13
GPF-Net w/ text	\checkmark	\times	29.54	20.63	42.81
GPF-Net w/ image	\times	\checkmark	59.91	67.85	82.64
GPF-Net (Ours)	\checkmark	\checkmark	68.86	80.17	89.62

Table 4. Compared to other object retrieval methods in terms of Params(M) and FLOPs(G).

Method	ViT [10]	CVRL [15]	VT-ReID [3]	DMCL [16]	GPF-Net (Ours)
Params	86.6	59.7	86.1	153.3	51.3
FLOPs	17.6	115	50.9	68.7	71.5

which is vital for polyp re-identification in general domain where the target supervision is not available.

3.5. Parameter Analysis

To go even further, we also elaborate a parameter analysis in Table 4, from which we can observe that GPF-Net can obtain a parameter value of 51.3M and 71.5G in terms of Params and FLOPs, which is significantly lower in terms of parameter quantity compared to existing mainstream methods, demonstrating excellent lightweight characteristics. Although the introduction of multimodal feature fusion has led to an increase in the model’s computational complexity, especially in terms of FLOPs, the extent of performance improvement far outweighs the rise in computational cost.

4. CONCLUSION

In this work, we present GPF-Net, a novel framework for colonoscopic polyp re-identification that addresses the limitations of single-stage multimodal fusion through a hierarchical gated progressive fusion strategy. By integrating a dynamic gating mechanism with multi-layer cross-modal interactions, our model effectively captures both fine-grained visual-text correlations and high-level semantic relationships. Importantly, our method ensures that complementary information from visual and textual modalities is progressively refined, from which we have proved that learning representation with multiple-modality can be competitive to methods based on unimodal representation learning. In the future, we will explore the interpretability of this method and apply it to other related computer vision tasks, *e.g.* polyp detection and segmentation.

5. REFERENCES

- [1] Yang Feng, Lin Ma, Wei Liu, and Jiebo Luo, “Spatiotemporal video re-localization by warp lstm,” in *CVPR*, 2019, pp. 1288–1297.
- [2] Qingzhong Chen, Shilun Cai, Crystal Cai, Zefang Yu, Dahong Qian, and Suncheng Xiang, “Colosrcl: Self-supervised contrastive representation learning for colonoscopic video retrieval,” *arXiv preprint arXiv:2303.15671*, 2023.
- [3] Suncheng Xiang, Cang Liu, Jiacheng Ruan, Shilun Cai, Sijia Du, and Dahong Qian, “Vt-reid: Learning discriminative visual-text representation for polyp re-identification,” in *ICASSP*. IEEE, 2024, pp. 3170–3174.
- [4] LANZ ALBERT, “A lite bert for self-supervised learning of language representations,” *arXiv preprint arXiv:1909.11942*, 2019.
- [5] Suncheng Xiang, Dahong Qian, Jingsheng Gao, Zirui Zhang, Ting Liu, and Yuzhuo Fu, “Rethinking person re-identification via semantic-based pretraining,” *ACM TOMM*, vol. 20, no. 3, pp. 1–17, 2023.
- [6] Kaiming He, Xiangyu Zhang, Shaoqing Ren, and Jian Sun, “Deep residual learning for image recognition,” in *CVPR*, 2016, pp. 770–778.
- [7] Liang Zheng, Liyue Shen, Lu Tian, Shengjin Wang, Jingdong Wang, and Qi Tian, “Scalable person re-identification: A benchmark,” in *ICCV*, 2015, pp. 1116–1124.
- [8] Zhedong Zheng, Liang Zheng, and Yi Yang, “Unlabeled samples generated by gan improve the person re-identification baseline in vitro,” in *ICCV*, 2017, pp. 3754–3762.
- [9] Wei Li, Rui Zhao, Tong Xiao, and Xiaogang Wang, “Deepreid: Deep filter pairing neural network for person re-identification,” in *CVPR*, 2014, pp. 152–159.
- [10] Mathilde Caron, Hugo Touvron, Ishan Misra, Hervé Jégou, Julien Mairal, Piotr Bojanowski, and Armand Joulin, “Emerging properties in self-supervised vision transformers,” in *ICCV*, 2021, pp. 9650–9660.
- [11] Giorgos Kordopatis-Zilos, Christos Tzelepis, Symeon Papadopoulos, Ioannis Kompatsiaris, and Ioannis Patras, “Dns: Distill-and-select for efficient and accurate video indexing and retrieval,” *IJCV*, vol. 130, no. 10, pp. 2385–2407, 2022.
- [12] Giorgos Kordopatis-Zilos, Symeon Papadopoulos, Ioannis Patras, and Ioannis Kompatsiaris, “Visil: Fine-grained spatio-temporal video similarity learning,” in *ICCV*, 2019, pp. 6351–6360.
- [13] Tengda Han, Weidi Xie, and Andrew Zisserman, “Self-supervised co-training for video representation learning,” *NeurIPS*, vol. 33, pp. 5679–5690, 2020.
- [14] Jie Shao, Xin Wen, Bingchen Zhao, and Xiangyang Xue, “Temporal context aggregation for video retrieval with contrastive learning,” in *WACV*, 2021, pp. 3268–3278.
- [15] Rui Qian, Tianjian Meng, Boqing Gong, Ming-Hsuan Yang, Huisheng Wang, Serge Belongie, and Yin Cui, “Spatiotemporal contrastive video representation learning,” in *CVPR*, 2021, pp. 6964–6974.
- [16] Suncheng Xiang, Hao Chen, Wei Ran, Zefang Yu, Ting Liu, Dahong Qian, and Yuzhuo Fu, “Deep multi-modal representation learning for generalizable person re-identification,” *Machine Learning*, vol. 113, no. 4, pp. 1921–1939, 2024.
- [17] Yanan Wang, Shengcui Liao, and Ling Shao, “Surpassing real-world source training data: Random 3d characters for generalizable person re-identification,” in *ACM MM*, 2020, pp. 3422–3430.
- [18] Binghui Chen, Weihong Deng, and Jiani Hu, “Mixed high-order attention network for person re-identification,” in *ICCV*, 2019, pp. 371–381.
- [19] Kuan Zhu, Haiyun Guo, Zhiwei Liu, Ming Tang, and Jinqiao Wang, “Identity-guided human semantic parsing for person re-identification,” in *ECCV*. Springer, 2020, pp. 346–363.
- [20] Hongchen Tan, Xiuping Liu, Yuhao Bian, Huasheng Wang, and Baocai Yin, “Incomplete descriptor mining with elastic loss for person re-identification,” *TCSVT*, vol. 32, no. 1, pp. 160–171, 2021.
- [21] Anguo Zhang, Yueming Gao, Yuzhen Niu, Wenxi Liu, and Yongcheng Zhou, “Coarse-to-fine person re-identification with auxiliary-domain classification and second-order information bottleneck,” in *CVPR*, 2021, pp. 598–607.
- [22] Haochen Wang, Jiayi Shen, Yongtuo Liu, Yan Gao, and Efstratios Gavves, “Nformer: Robust person re-identification with neighbor transformer,” in *CVPR*, 2022, pp. 7297–7307.
- [23] Guanshuo Wang, Yufeng Yuan, Xiong Chen, Jiwei Li, and Xi Zhou, “Learning discriminative features with multiple granularities for person re-identification,” in *ACM MM*, 2018, pp. 274–282.
- [24] Xuesong Chen, Canmiao Fu, Yong Zhao, Feng Zheng, Jingkuan Song, Rongrong Ji, and Yi Yang, “Salience-guided cascaded suppression network for person re-identification,” in *CVPR*, 2020, pp. 3300–3310.